Modelling sound propagation in the ocean: a normal mode approach using finite elements

Ray Kirby (1), Wenbo Duan (2)

(1) Centre for Audio, Acoustics and Vibration, University of Technology Sydney, Sydney, Australia
(2) Brunel Innovation Centre, Brunel University London, London, United Kingdom

ABSTRACT

Modelling the propagation of sound waves in the ocean is challenging because one must account for spatial variation in properties of the fluid and in the ocean geometry, as well as couple the fluid to a seabed that supports both shear and compressional waves. This article presents a finite element based approach to obtaining the eigenmodes for an axial uniform ocean waveguide. Once these modes have been computed, an orthogonality relation is used to compute the sound pressure field for ranges of up to 5 km. This approach avoids the traditional heavy computational expenditure associated with the finite element method, at least for a uniform waveguide. Furthermore, the numerical approach properly accounts for the depth dependent properties of the ocean, and couples the ocean to a full elastodynamic representation of the seabed, which supports both shear and compressional waves. This permits the implementation of the physically correct transverse boundary conditions, as well as the addition of a perfectly matched layer to enforce the correct boundary conditions at infinite depth in the seabed.

1 INTRODUCTION

Developing a mathematical model suitable for analysing sound propagation in the ocean presents a considerable challenge. This relates to the size and complexity of a typical ocean environment and so it is common to explore different ways to try and simplify the problem. One popular approach is to reduce the problem to a two dimensional uniform waveguide and to then compute the normal modes for the guide. This approach was pioneered by Pekeris (1946) and many different variations have followed, see Etter (2013) for a comprehensive review. A typical normal mode solution does however contain many approximations and many additional challenges also need to be addressed. The most significant of these include the variation of density and sound speed in the ocean, as well as coupling the ocean to the seabed. To address these problems, the ocean waveguide literature generally adopts an analytic approach and here the use of ray tracing is popular because of the size of the ocean and the typical frequency range encountered, see for example discussions of various ray tracing methods by Etter (2013), as well as discussions on the use of parabolic equations. One of the most popular examples is the normal mode approach of Westwood et al. (1996), which is commonly referred to as the ORCA model. This approach is a comprehensive analysis that attempts to account for the changes in fluid density, as well as coupling the ocean to an elastic representation of the seabed. The approach relies on separating the guide into multiple ducts in which the sound speed is either constant or varies linearly; the method also introduces some assumptions about interactions at the interface between an elastic solid and a fluid. Moreover, the method also relies on analytic expansions and so this will make the problem progressively more challenging as the frequency is increased. This makes it very difficult to properly capture the terminating boundary condition at the bottom of the seabed, in the limit that the seabed tends to infinity. Nevertheless, the analytic normal mode method of ORCA is often used as a benchmark solution and is considered to provide a good approximation of true performance, as well as delivering solutions in a relatively short timescale.

This article introduces an alternative approach to obtaining a modal solution for a uniform ocean waveguide. The approach is based on the so-called semi-analytic finite element (SAFE) method that has been developed in the structural mechanics and acoustics literature. The method involves expanding the unknown variables in the axial direction of the waveguide as an infinite sum over the guide eigenmodes in the usual way, but then uses the finite element method to discretise the guide in the transverse direction in order to solve the eigenproblem numerically. This method has been used to obtain eigenmodes for elastic waveguides, see for example Duan and Kirby (2015). More recently the method has been extended to buried pipelines (Duan et al. 2016) and fluid filled buried pipes, Kirby et al. (2017) and Kalkowski et al. (2018). This approach for buried pipelines has seen the development of

an efficient one dimensional method that makes use of a perfectly matched layer to accommodate the boundary condition at infinity in the surrounding [elastic] material, which is often soil or sand. It is interesting to note that the problem analysed in fluid filled buried pipes is very similar to the one being addressed in ocean waveguides: there exists a region of fluid that is coupled to an elastic structure and then to another elastic structure in which a transverse boundary condition must be applied at infinity. Accordingly, the SAFE method offers an interesting alterative approach for obtaining the eigenmodes of an acousto-elastic environment.

The advantage of the SAFE method is that by using a numerical discretisation of the problem one may easily account for variations in fluid density (and sound speed). Furthermore, one can properly enforce the continuity conditions between the fluid and the seabed without any accompanying approximations, as well as enforce the appropriate transverse boundary condition within the seabed. This can be achieved with a method that is fast and efficient and so has the potential to address larger ocean waveguide problems. Accordingly, this article describes the underlying concept behind the application of the SAFE method to ocean acoustics, and shows that the method can be used to plot the acoustic pressure in an ocean environment. However, a full derivation of the mathematics that supports this analysis is rather lengthy and so this will be reported elsewhere.

2 Theory

A schematic of the ocean waveguide is presented in Fig. 1.

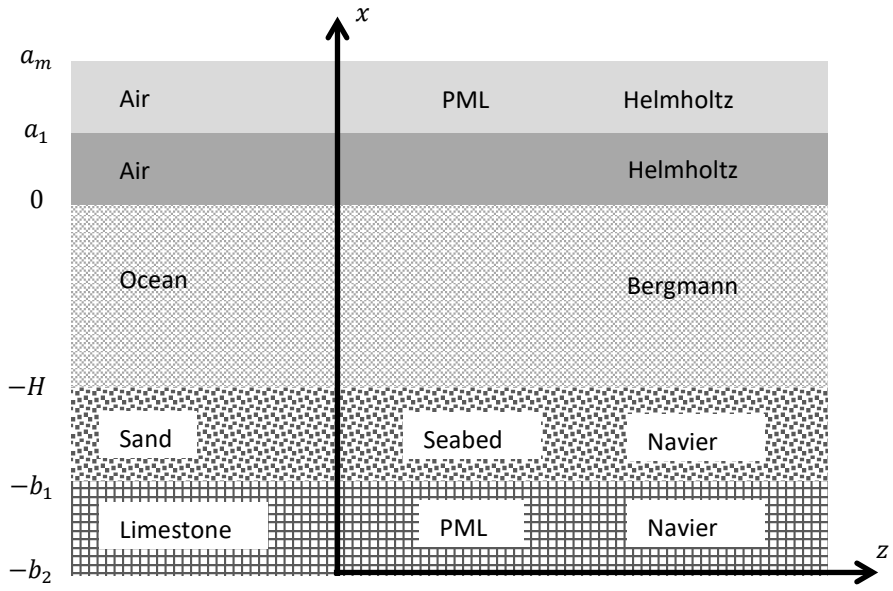

Figure 1: Geometry of waveguide with governing PDE.

The waveguide is intended to fully characterise the problem and so includes air above the ocean, which is then coupled to seawater in which the density and sound speed may change continuously with depth. The seawater is then coupled to an elastic seabed in which two layers are included. The first layer in this article is chosen to be sand and the second layer limestone for most of the predictions that follow; however, the choice of material is entirely arbitrary. Note that damping or absorption can easily be included in any of the layers shown in Fig. 1.

Each fluid region is modelled using the acoustic wave equation, which for variable density is given by the Bergmann equation (Bergmann 1946)

$$\rho_f \nabla \cdot \left(\frac{1}{\rho_f}\nabla p'\right) - \frac{1}{c_f^2}\frac{\partial^2 p'}{\partial t^2} = 0. \tag{1}$$

This equation reduces to the well-known Helmholtz equation in regions of constant density (after substituting in the time dependence). Here, p' is the acoustic pressure, and ρ_f and c_f are the density and speed of sound in the

fluid, respectively. For a solid region the elastodynamic wave equation is used, which is also known as Navier's equation, and this is given as

$$(\lambda+\mu)\nabla(\nabla\cdot\boldsymbol{u}')+\mu\nabla^2\boldsymbol{u}'=\rho\frac{\partial\boldsymbol{u}'}{\partial t^2} \tag{2}$$

In the solid, λ and μ are the Lamé constants, ρ is the density and $\boldsymbol{u}'$ is the displacement vector. The relevant boundary conditions are:

$$\left[\frac{\partial}{\partial x}-ik_f\right]p'=0;\quad x\to+\infty. \tag{3}$$

$$p'_{\text{air}}=p'_{\text{ocean}}\quad\text{and}\quad v'_{x,\text{air}}=v'_{x,\text{ocean}};\quad x=0. \tag{4}$$

$$p'_{\text{ocean}}=-\sigma'_{xx}\quad\text{and}\quad v'_{x,\text{ocean}}=u'_x=;\quad x=-H. \tag{5}$$

$$\sigma'_{xx}=\sigma'_{xz}=0\qquad x\to-\infty. \tag{6}$$

Here, v'_x is the acoustic velocity in the x direction in either the air or the ocean, and σ'_{jk} is a stress tensor. Additional boundary conditions also apply at the interface between air and seawater, and the two layers in the seabed, however these boundary conditions can be applied naturally thought the finite element discretisation provided each governing equation is scaled appropriately. The boundary conditions at $x\to+\infty$, and $x\to-\infty$ are applied using perfectly matched layers (PMLs), which make use of complex coordinate stretching functions, so that

$$\tilde{x}=\int_0^x\xi(s)ds \tag{7}$$

where values for $\xi(s)$ are chosen to ensure that the boundary conditions are enforced in the most computationally efficient way. For example, Duan et al. (2016) show that through the appropriate choice of $\xi(s)$, the PML can be attached directly to the first layer of an elastic solid, so that in Fig. 1 the PML would start at $x=-b_1$. This facilitates a reduction in the size of the PML and so enables the development of a fast and efficient way of enforcing the terminating boundary conditions.

To solve the problem, the acoustic pressure and the displacement in the solid are expanded over the (coupled) waveguide eigenmodes to give

$$p'(x,z;t)=\sum_{m=0}^{\infty}A_m p_m(x)e^{i(\omega t-k_m z)} \tag{8}$$

$$\boldsymbol{u}'(x,z;t)=\sum_{m=0}^{\infty}A_m\boldsymbol{u}_m(x)e^{i(\omega t-k_m z)} \tag{9}$$

Here, p_m and $\boldsymbol{u}_m$ are the eigenvectors, and k_m are the eigenvalues, for the coupled problem. In addition, A_m are the modal amplitudes. The substitution of Eqs. (8) and (9) back into the governing equations and the addition of the boundary conditions enables, after some effort, one to write the problem as a standard eigenequation that can be solved for p_m, $\boldsymbol{u}_m$ and k_m. This is accomplished using a standard finite element discretization, which can easily accommodate a change in the density of the fluid (and the solid if so desired).

Finally, this article also plots the acoustic pressure in the waveguide and to do this it is necessary to compute the modal amplitudes A_m. In this article a monopole source is used to excite the waveguide, and this enables the modal amplitudes to be found using the following expression:

$$A_m=\frac{Q_s\rho_f(x_s)c_m p_m(x_s)}{\Lambda_{mm}}. \tag{10}$$

Here, Q_s is the monopole source strength, $\rho_f(x_s)$ is the density of the fluid at the location of the source $x=x_s$ (which is assumed to lie in the fluid); c_m is the modal phase speed and Λ_{mm} is an appropriate orthogonality relation (Scandrett and Frenzen 1995).

3 RESULTS

Results are presented here for the geometry and material properties used by Westwood et al. (1996) in their ORCA paper, see Tables 1 and 2. However, variations in density and the speed of sound within the fluid are taken from Fahy and Walker (1998).

Table 1: Dimensions of waveguide

Parameter	Value
a_m *(m)*	8
a_1 *(m)*	4
H *(m)*	200
b_1 *(m)*	210
b_2 *(m)*	230

Table 2: Properties of elastic materials

Parameter	Sand	Limestone	Concrete
μ *(GPa)*	0.224+0.000713i	3.987+0.00633i	16
λ *(GPa)*	3.3635+0.00464i	6.421-0.00122i	9
Density, ρ *(kg/m^3)*	1400	2300	2300

In Figure 2, the mode shapes for the first four modes in which the acoustic energy lies predominantly in the seawater are presented at a frequency of 50 Hz.

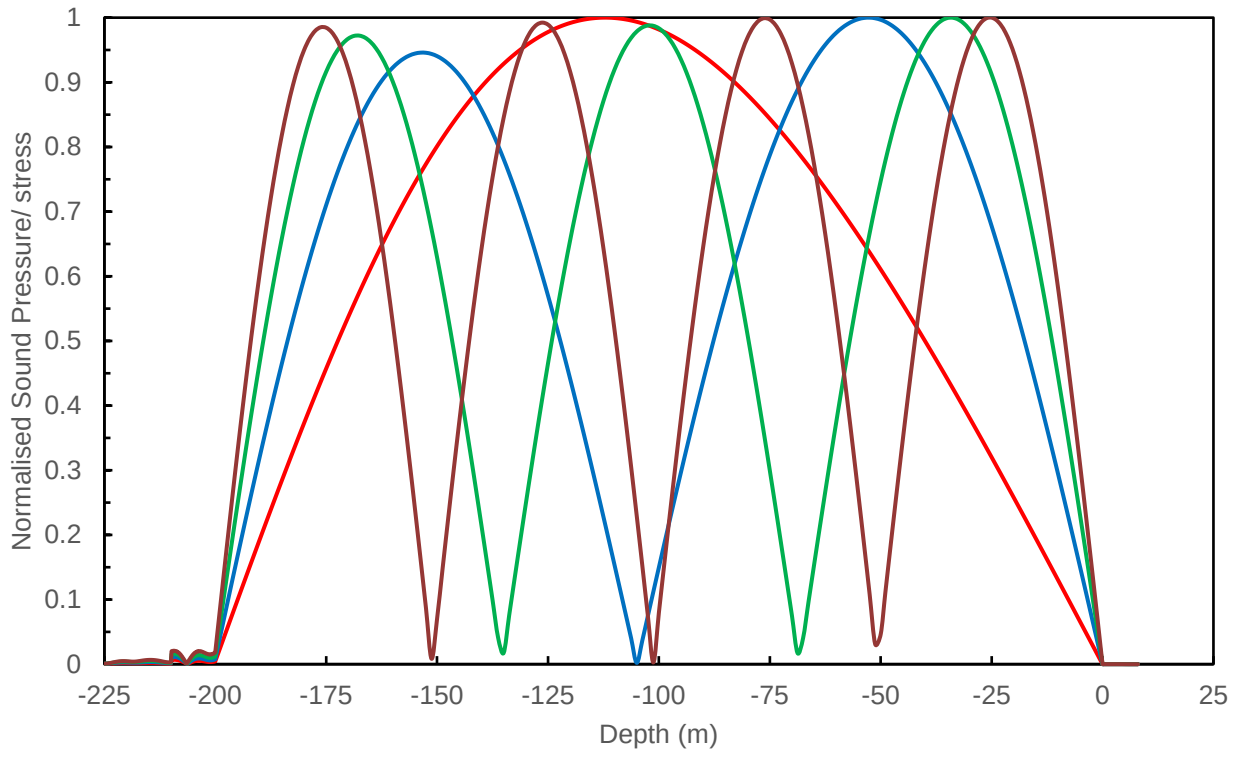

Figure 2: Mode shapes for pressure/σ_{xx} at 50 Hz for the first four modes with energy concentrated in the seawater.

The modes in Fig. 2 have been sorted from those in which the energy lies either in the air or the seabed. Figure 2 shows a reasonably standard profile and it is seen that the approximate boundary condition of zero acoustic pressure at the top and bottom of the seawater generally holds. However, it is noted that this only applies to these fluid type modes, and one can also see that as the mode order increases the zero pressure boundary condition becomes progressively more inaccurate at the seafloor. Figure 2 also illustrates the enforcement of the relevant boundary conditions in the respective PMLs in the air and the seabed.

In Figure 3 the transverse displacement (x direction) is shown for the same problem as that studied in Fig 2. The solid line represents the solution with the PML present in the model, and overlaid on top of this is the equivalent solution obtained using the geometry and material properties in the ORCA model (Westwood et al. 1996). In the ORCA model, the boundary condition in the seabed is approximated by using a very deep section of limestone with very heavy damping. It is easy to replicate this geometry with the SAFE method, and so it is the SAFE predictions that appear in Fig 3 (and not predictions taken using the ORCA solution). Thus, Figure 3 illustrates the physical limitations of the way in which ORCA enforces the boundary conditions in the seabed.

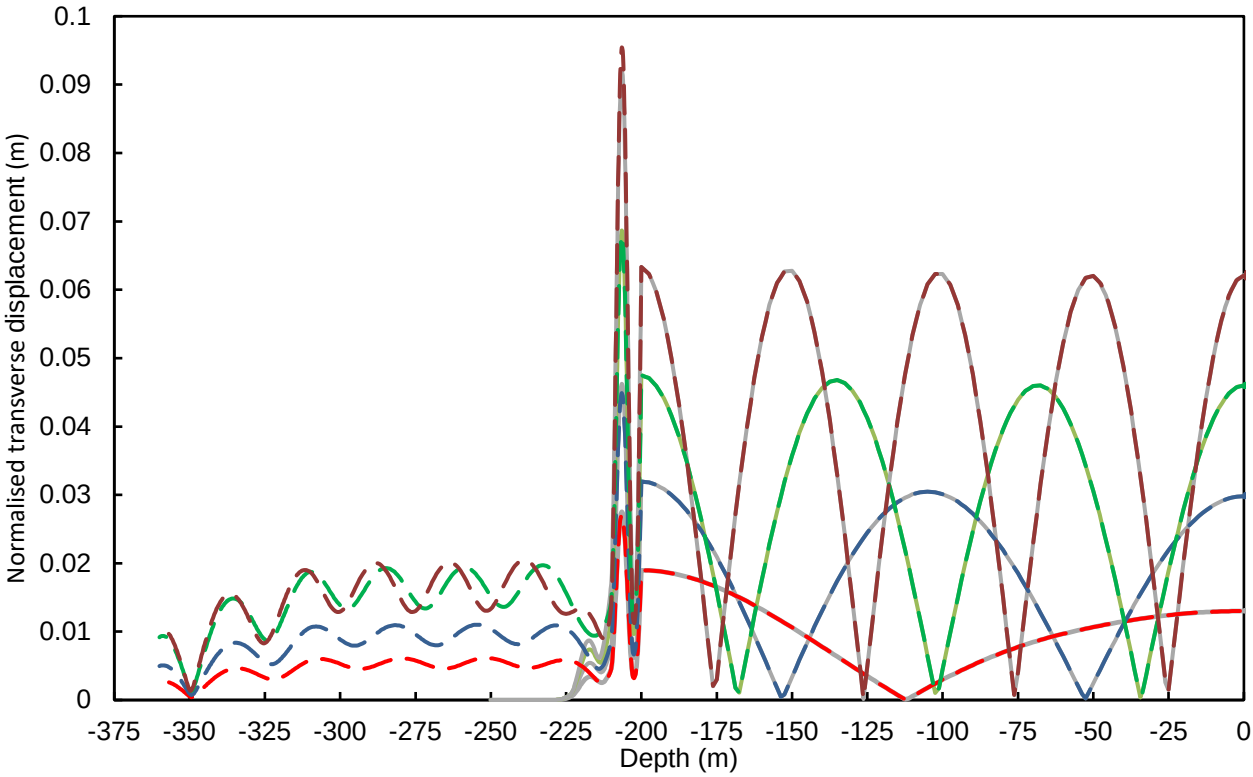

Figure 3: Mode shapes for displacement at 50 Hz for the first four modes with energy concentrated in the seawater. Solid lines, SAFE + PML; dashed lines, SAFE with ORCA boundary condition in seabed.

In Fig. 3 it can be seen that in principle the modes shapes within the fluid region can be obtained accurately, however the boundary condition applied in ORCA is only an approximation in the lower section of the seabed and this is observed in the incorrect limiting behaviour of the displacement. In contrast, the PML is seen to properly enforce this boundary condition and does this quickly and efficiently over a short distance.

The modal solutions obtained from the eigenproblem can be used to find the sound pressure distribution in the axial direction using Eq. (10) for a given number of modes, M, and these are chosen to deliver convergence in the sound pressure distribution. In Fig. 4 the sound transmission loss at $x = -150$ m for a sound source placed at $x_s = -50$ m is shown for various different mesh densities and values of M, at a frequency of 50 Hz (for the example studied previously). The sound transmission loss follows the usual definition (Westwood et al. 1996).

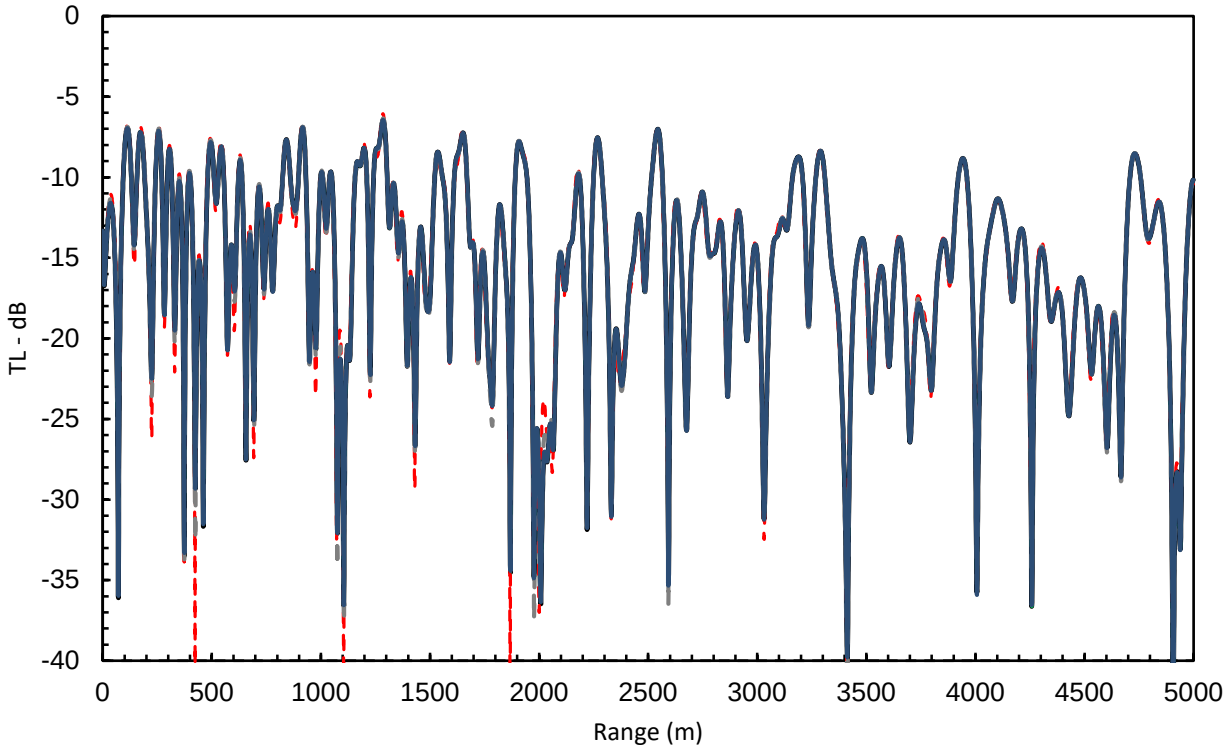

Figure 4: Convergence of predictions for sound transmission loss at 50 Hz with source at -50 m and receiver at -150 m.

In Fig.4, three different solutions are obtained, and these range from 950 to 2826 degrees of freedom (eigenmatrix order), and with $M = 50, \text{or } 150$. It can be seen in Fig. 4 that all three solutions overlay one another and this illustrates that convergence for this problem is readily achieved for a relatively modest problem size, at least at this frequency.

One of the main advantages of the SAFE method is that it can properly account for the coupling between the ocean and the seabed, including implementing the appropriate boundary at $x = -\infty$. Clearly, the effect of this coupling will become progressively more important for shallower oceans and it is here that the advantages of the SAFE approach are likely to become more pronounced. For example, the influence of the seabed on sound transmission loss is illustrated in Fig. 5, for a waveguide of depth $H = 25$ m. In Fig. 5 the solid black line is the reference solution taken using the properties of the seabed described in the previous examples (Westwood et al. 1996), but with $b_1 = 35$ m and $b_2 = 85$ m. The solid grey line is for the same dimensions as the first case, but this time replacing limestone with concrete (see Table 2). The final case, which is the dashed line, increases the depth of sand to 30 m and has a 50 m layer of concrete below the sand. It can be seen in Fig. 5 that the sound transmission loss changes significantly with different properties in the seabed. This is to be expected because in this particular example the coupling between the fluid and the solid is strong. This illustrates the ability of the SAFE method to capture the changes in behaviour associated with the conditions present in the seabed, however it also illustrates that the predictions are likely to be very sensitive to the acoustic properties used to represent each material, at least for shallower waveguides.

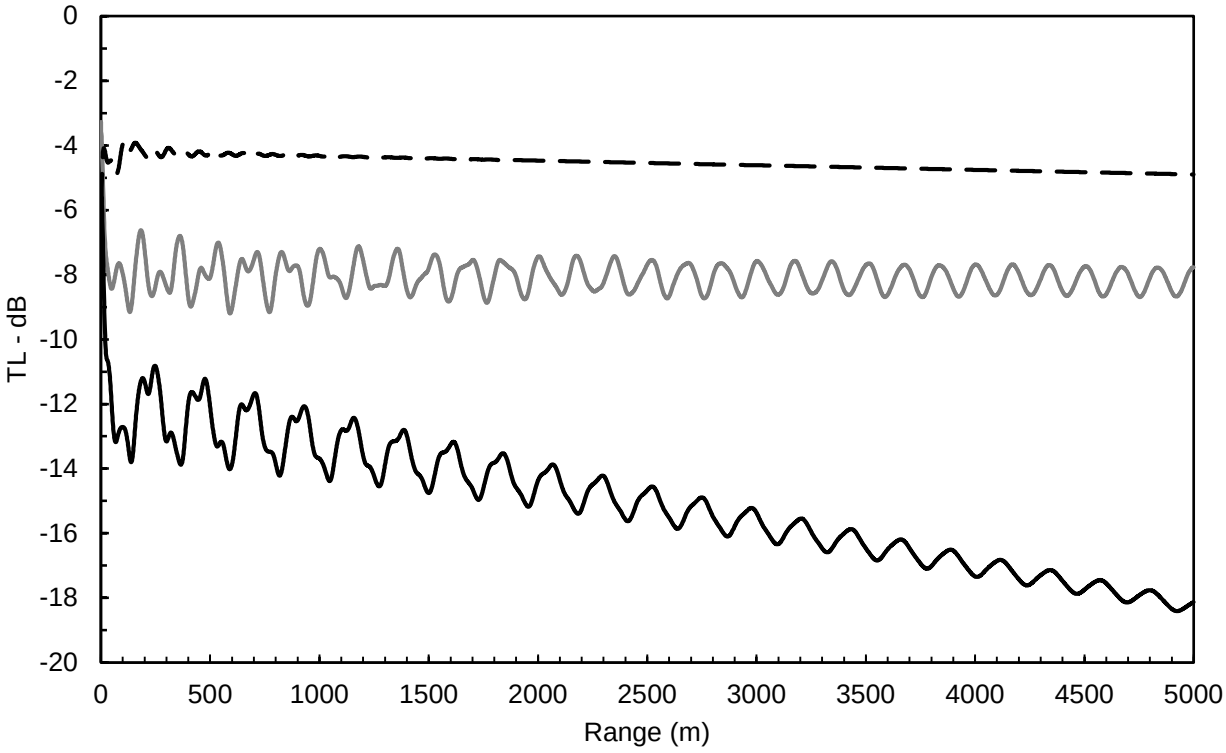

Figure 5: Transmission loss at 50 Hz for with source at -10 m and receiver at -20 m.
———, seabed of sand with depth 10 m and limestone of depth 50 m;
———, seabed of sand with depth 10 m and concrete of depth 50 m;
– – – –, seabed of sand with depth 30 m and concrete of depth 50 m.

Finally, in Figs. 6-8, the sound pressure level generated by a monopole source is presented for an ocean waveguide at different frequencies. The sound pressure level is normalised against the source strength. In Figs. 6-8 the geometry used in the ORCA model (Table 1) is used, as well as sand and limestone (Table 2). The sound pressure distribution at 50 Hz is plotted in Fig. 6, with 250 Hz in Fig. 7, and 500 Hz in Fig. 8.

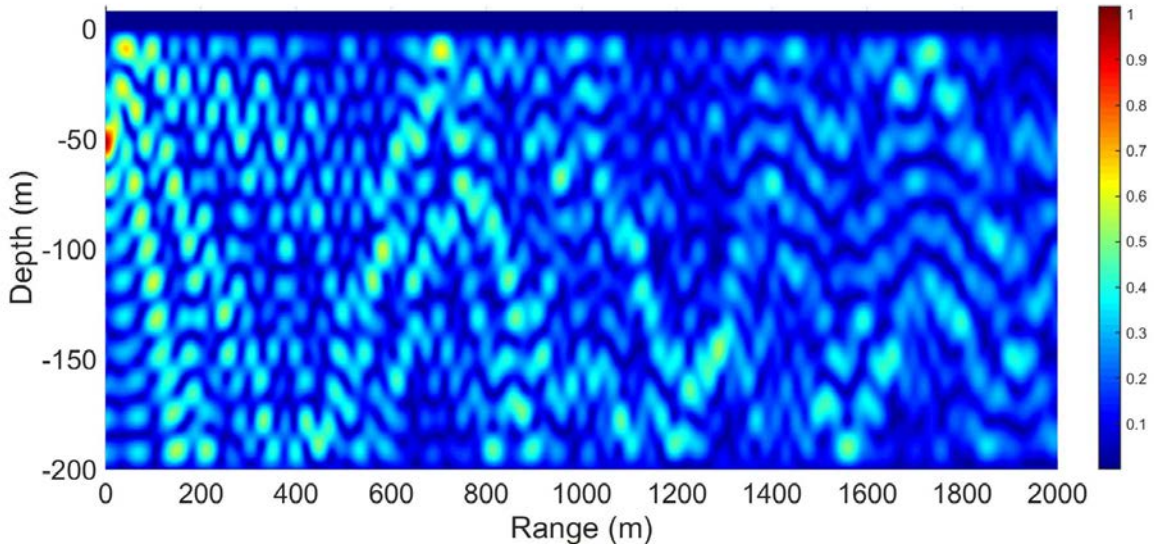

Figure 6: Normalised sound pressure level at 50 Hz using 50 modes.

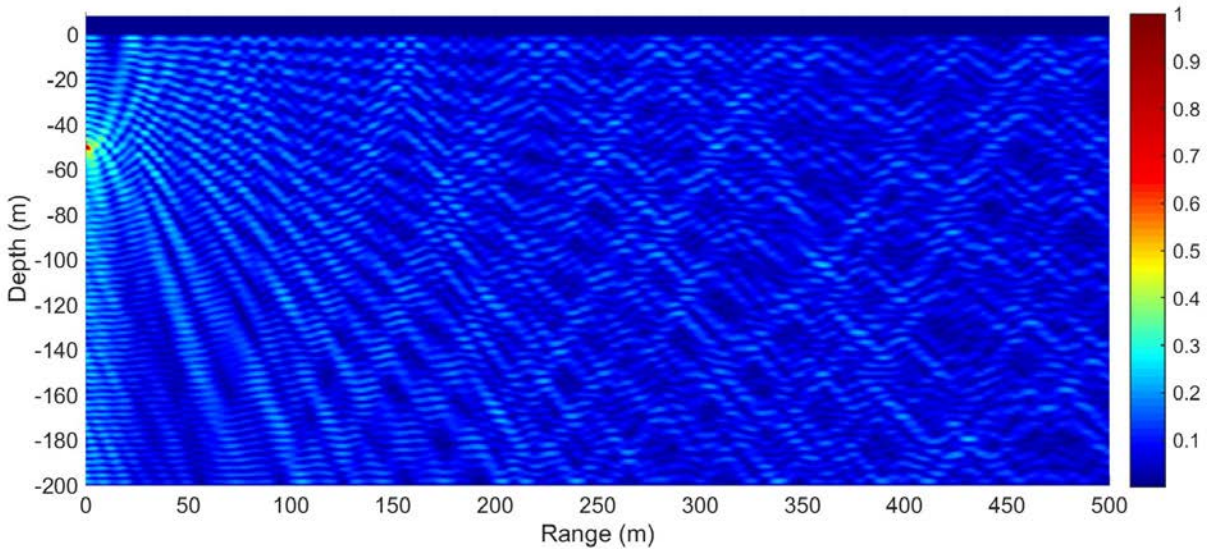

Figure 7: Normalised sound pressure level at 50 Hz using 250 modes.

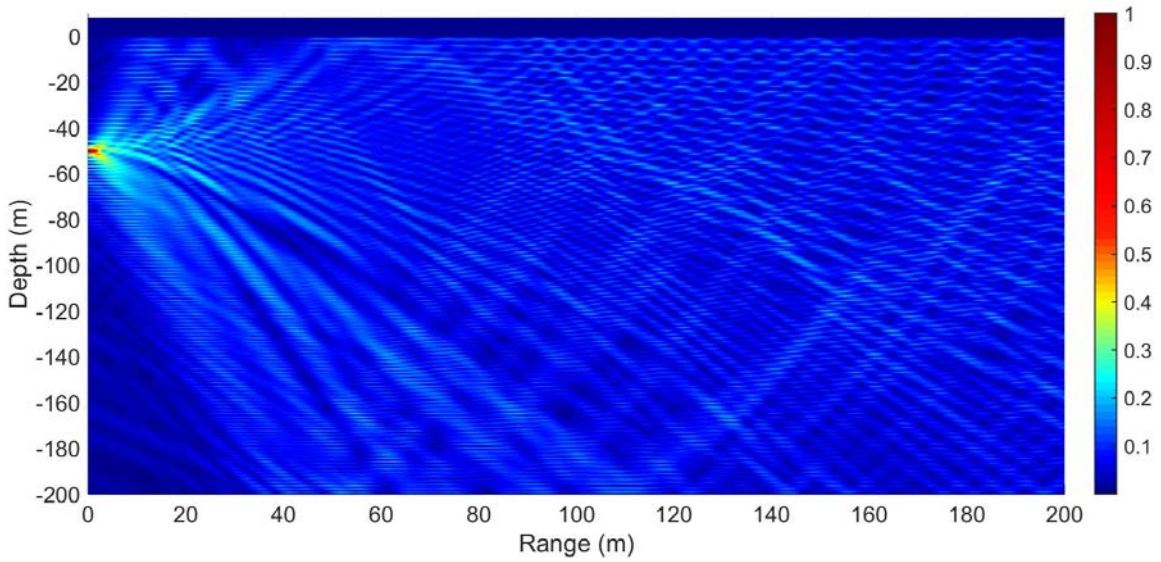

Figure 7: Normalised sound pressure level at 50 Hz using 400 modes.

It is reminded here that in Figs. 6-8, these pressure plots have been obtained without discretisation in the axial direction (range). All that is required is the one dimensional mesh in the x-coordinate at $z = 0$. This means that the time taken to solve the problem is also independent of the range that is plotted, and here the range is reduced for the higher frequencies only in order to show up detail. Accordingly, these plots can be generated relatively quickly, so that each of these pressure plots takes between about 1 and 2 seconds to generate on a standard laptop computer (using MATLAB®). This speed can be improved upon for real applications once one has decided upon the tolerance levels/errors that are acceptable for a particular application. Note also that when generating plots of sound pressure it is not necessary to sort the modes into different categories. Each mode will be excited according to their mode shape, so that some modes that have energy lying predominately in the sold, or air, will not be strongly excited by a monopole source in the seawater. This means that the modal amplitude for these modes will be small and they will not contribute to the final sound pressure plots. That is, this method does not require one to spend time sorting through each mode type and distinguishing say, Scholte and Stoneley waves

from other types of waves. All that is necessary is that a sufficient number of modes are retained when computing sound pressure level to achieve a converged solution, and the numbers used are listed on Figs. 6-8. Of course, as the frequency increases, then the number of modes required will also increase and the problem will become progressively more challenging.

The sound pressure distributions seen in Figs. 6-8 generally exhibit the behaviour expected in ocean waveguides, especially in terms of the diffraction of the propagating sound field. This article is designed to demonstrate the ability of the model to generate sound pressure plots and of course it remains for these predictions to be benchmarked in the future.

4 CONCLUSIONS

The purpose of this article is to demonstrate that finite elements can be used to generate sound pressure distributions for ocean waveguides without the use of large numbers of elements. The SAFE method requires only the transverse (depth) dimension to be meshed and, provided one uses an appropriate orthogonality relation, it is then straightforward to calculate the amplitudes of each mode and to recover the sound pressure distribution. This means that the approach is computationally fast and efficient, and sound pressure plots can generally be recovered in under 10 seconds for frequencies up to 500 Hz. A key advantage of the SAFE method is that one can readily include depth dependence for fluid density and sound speed in the ocean, as well as properly capture the continuity conditions between the ocean and the seabed and accurately enforce the appropriate boundary conditions at the bottom of the seabed.

This approach does, of course, depend on the assumption of a uniform ocean waveguide, and so the SAFE method should be seen as complementary to those analytic methods that investigate the normal mode problem. However, the speed of the method means that it is capable of going to higher frequencies and it is possible that the method could also supplement some ray acoustics models as well. Furthermore, it has been shown in articles on pipelines (Duan et al. 2017) that a fast and efficient frequency domain method can then be used to compute time domain predictions, so that the approach presented here has the potential for studying wave propagation in the ocean in the time domain.

The computation of normal modes in a two dimensional waveguide is only an approximation of the true problem. However, once one has found the eigenvalues for a uniform section of the ocean, it is possible to extend this analysis to discontinuities, or finite regions in which a non-uniform section is present. For example, for uniform discontinuities, say when an ice sheet is present, mode matching can be used to join uniform regions together, see Kirby et al. (2014) and Duan et al. (2017). For non-uniform sections, one can also use mode matching to join modal solutions for uniform sections to a full finite element discretisation of non-uniform sections using a so-called hybrid method, see Kirby (2008) and Duan and Kirby (2015). This method provides an approach to minimising regions in which it is necessary to apply a full finite element discretisation, and so offers the potential to reduce problem size and hence generate more accurate predictions over a wider frequency range, even for more complex geometries than those discussed in this article.

REFERENCES

Bergmann, P.G. 1946. ‘The wave equation in a medium with a variable index of refraction’. *Journal of the Acoustical Society of America* 17: 329-333.

Duan, W., Kirby, R. 2015. ‘A numerical model for the scattering of elastic waves from a non-axisymmetric defect in a pipe’. *Finite Elements in Analysis and Design* 100: 28-40.

Duan, W., Kirby, R., Mudge, P., Gan, T-H. 2016. ‘A one dimensional numerical approach for computing the eigenmodes of elastic waves in buried pipelines’. *Journal of Sound and Vibration* 384: 177-193.

Duan, W., Kirby, R., Mudge, P. 2017. ‘On the scattering of torsional waves from axisymmetric defects in buried pipelines.’ *Journal of the Acoustical Society of America* 141: 3250-3261.

Etter, P.C. 2013. Underwater acoustic modelling and simulation. 4th ed. London: CRC Press, Taylor and Francis Group.

Kalkowski, M.K., Muggleton, M.J., Rustighi, E. 2018 ‘Axisymmetric semi-analytical finite elements for modelling waves in buried/submerged fluid-filled waveguides’. *Computers and Structures* 196: 327-340.

Kirby, R. 2008. ‘Modeling sound propagation in acoustic waveguides using a hybrid numerical method’. *Journal of the Acoustical Society of America* 124: 1930-1940.

Kirby, R. Williams, P.T., Hill, J. 2014. 'A three dimensional investigation into the acoustic performance of dissipative splitter silencers'. *Journal of the Acoustical Society of America* 135: 2727-2737.
Kirby, R., Duan, W., Karimi, M., Brennan, M., Kessissoglou, N. 2017 'Detecting sound waves generated by leaks in buried water distribution pipes'. *Proceedings of Acoustics 2017*, Perth, Australia.
Fahy F., Walker J. 1998. Fundamentals of noise and vibration. London: E & FN Spon
Nguyen K.L, Treyssède F., Hazard C. 2015. 'Numerical modeling of three-dimensional open elastic waveguides combining semi-analytical finite element and perfectly matched layer methods'. *Journal of Sound and Vibration*: 344: 158 – 178.
Pekeris, C.L. 1946. 'Theory of propagation of sound in a half-space of variable sound velocity under conditions of formation of a shadow zone'. *Journal of the Acoustical Society of America* 18: 295–315.
Scandrett, C.L., Frenzen, C.L. 1996. 'Bi-orthogonality relationships involving porous media'. *Journal of the Acoustical Society of America* 98: 1199-1203.
Westwood, E.K., Tindle, C.T., Chapman, N.R. 1996. 'A normal mode model for acousto-elastic ocean environments'. *Journal of the Acoustical Society of America* 100: 3631–3645.